LINEAR STABILITY OF A COMPRESSIBLE BINARY SHEAR LAYER

Leonardo da Costa Salemi, leonardo.salemi@embraer.com.br
Empresa Brasileira de Aeronáutica S.A.

Márcio Teixeira de Mendonça, marcio@iae.cta.br
Comando Geral de Tecnologia Aeroespacial - Instituto de Aeronáutica e Espaço

Abstract. *Many aerospace systems rely on the release of chemical energy to work properly. Among the most usual applications are aircraft and rocket engines. Understanding how the mixing occurs inside the combustion chamber is very important on the design and prediction of performance of such propulsion systems. On supersonic combustion this knowledge is crucial as the short residence times require eficient mixing. Linear stability analysis (LSA) provides significant and accurate insight into the flow physics at negligible computational cost. It is used herein to study the stability of the compressible binary mixing layer. Stability analysis begins with the 2-D viscous compressible binary flow variables' laminar profile calculation via the conservation equations transformed to obtain a similar solution for the mixing layer. With the similar solutions, the conservation equations for a 3-D inviscid compressible binary laminar flow subjected to infinitesimal disturbances are derived. A normal mode form solution is proposed leading to an eigenvalue problem. The results show that variations of the Chapman-Rubesin parameter, Prandtl and Lewis numbers across the mixing layer should be taken into account in the calculations as they affect the base flow profiles and also temporal growth rates. Curves for the variation of the temporal amplification rate against wave number for convective Mach number ranging from 0.01 to 1.6 are presented.*

Keywords: *Hydrodynamic, Stability, Mixing, Compressible, Combustion*

1. INTRODUCTION

In the beggining of atmospheric flight era, flying devices couldn't reach neither very high altitudes nor high speeds. It was during the space age that the first hypersonic vehicles were developed. Flight in the hypersonic regime requires other technologies than the ones used by subsonic or supersonic aircraft, like special airframe cooling, shapes tailored to stand extreme temperatures due to aerodynamic heating and mainly, more efficient propulsive devices capable of generating enough thrust throughout distinct regimes of flight.

Ramjets use the ram pressure of the surrounding gas and its passage through a diffuser, a combustion chamber and a nozzle to generate thrust (Fig.1). When the working fluid passes through the diffuser it is deccelerated from supersonic to subsonic speeds. Therefore, the combustion process happens under the subsonic regime. Later on, the gases are accelerated in a convergent/divergent nozzle, being exhausted above $M = 1$.

Scramjets work on the same fashion as ramjets, but the combustion process is supersonic inside the combustion chamber (Fig.2). The combustion has to be supersonic, otherwise the high kinetic energy of the flow would be lost if the gas were to be decelerated from supersonic to subsonic speeds before the chemical reaction starts. The products of combustion are also exhausted above $M = 1$, but on a divergent nozzle.

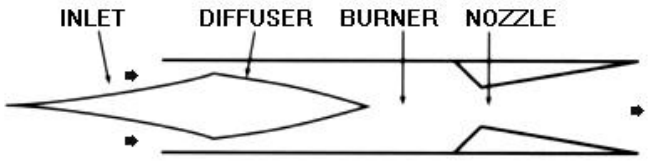

Figure 1. Schematic view of a ramjet engine (Merry, 2006)

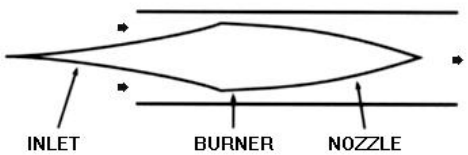

Figure 2. Schematic view of a scramjet engine (Merry, 2006)

Within a ramjet/scramjet combustion chamber, the fuel injection process can be simplified and modelled as a plane shear layer flow, considering that both the oxidizer and fuel are gases.

A shear layer appears when two gases initially separated by a splitter plate are brought together creating an interface. This interface is formed due to the flow properties' gradients (i.e. velocity, temperature, species concentration) between both layers of fluid. Small disturbances (i.e. infinitesimal) generated by acoustic waves, residual turbulence on both flows or surface roughness of the splitter plate, are amplified . This amplification phenomena results in the formation of large vortical structures (Winant and Browand, 1974; Brown and Roshko, 1974), which evolve to transition and later to turbulence. A shear layer sketch can be visualized on Fig.3.

In order to understand how the small disturbances of the flow affect a reactive shear layer evolution, Shin and Ferziger

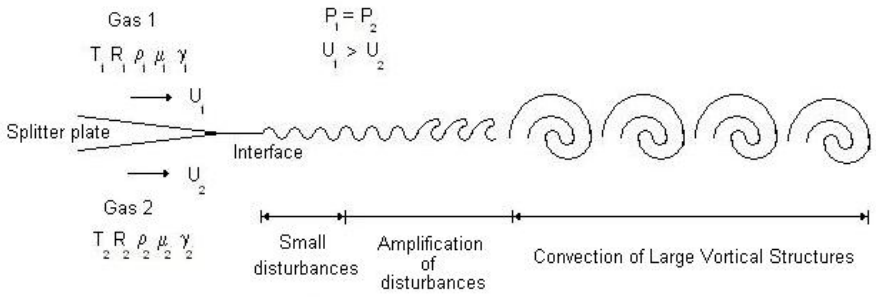

Figure 3. Sketch of a binary shear layer (Salemi, 2006)

(1991) presented temporal and spatial growth rates considering constant and variable thermodynamic and transport properties' formulation. They noticed that the constant property formulation affects both temporal and spatial growth rates. In a later study, Kennedy and Gatski (1994) showed that these physical properties' variation can be quite high depending on which gases are present on each layer. As pointed out by Kozusko et al. (1996) the binary shear layer base flow solution is also highly dependant on the two gases considered. Recently, Fedioun and Lardjane (2005) provided numerical data that also show the dependence on the flowing gases of the stability characteristics of a compressible shear layer.

Shin and Ferziger (1991) used Prandtl and Lewis numbers equal to unity in their formulation and claimed that $Pr = 0.7$ did not produce large quantitative differences, but do not present any data supporting this claim. They also have used an implicit method (Crank-Nicholson) to solve the boundary layer equations. Herein, it is used a similar transformation and a similar solution for the conservation equations is sought. It is shown that, although using the Chapman-Rubesin parameter, Prandtl and Lewis numbers equal to unity simplifies the equations to be solved, variations in these parameters do produce significant quantitative differences in terms of laminar base flow profiles and temporal growth rates for a compressible binary shear layer. In addition, some calculated data through LSA for a compressible binary shear layer for convective Mach number ranging from 0.01 to 1.6 are presented.

2. FORMULATION

In this section it is presented the formulation used for the calculations performed. It is detailed how the thermodynamic properties and transport coefficients are calculated and also the equations and boundary conditions used to calculate the laminar base flow and to perform the linear stability analysis.

In order to study the shear layer problem, some definitions must be made. Granted that a velocity difference exists between the upper and lower layers, a velocity profile as shown on Fig. 4 is present. Along the present work, it is assumed that the splitter plate's wake is negligible and that it divides the shear layer in upper and lower layers. This division is solely a definition as there is no symmetry between the layers. It is also to define where is located the origin of the coordinated axis (x axis) in order to pose the third boundary condition ($v(0) = 0$).

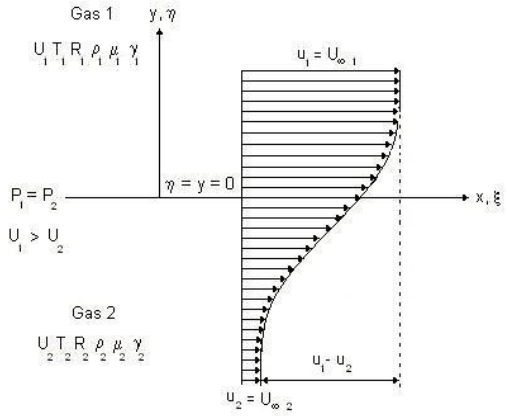

Figure 4. Velocity profile on a binary shear layer (Salemi, 2006)

Let U_1 be the velocity of the freestream in the upper layer in the x direction and U_2 be the velocity of the freestream in the x direction for the lower layer. As shown in Fig. 4, $U_1 > U_2$. Therefore, the upper layer, 1, is called fast layer, and the lower layer, 2, is called the slow layer. Herein, are presented only cases where $U_1 > U_2$. It is also worthy to mention that, as the system is binary, the fast layer's component is always written before the slow layer's component. So, the binary

shear layer composed of Hydrogen, H_2, as upper layer and Nitrogen, N_2, as lower layer is identified as a H_2 - N_2 layer.

2.1 Thermodynamic properties and transport coefficients

For the plane compressible binary shear layer it is considered that $p_1 = p_2 = p$. Therefore, the pressure on both layers is the same throughout the shear layer and the gases follow Amagat law (Van Wylen et al., 1994). Density (ρ) calculations follow from this law.

Both gases are treated as a binary mixture in which the physical properties are calculated depending on the local mass/molar fraction of the chemical species. Viscosity and thermal conductivity for each of the species is calculated using the temperature polynomial functions presented in the work of Svehla (1995) and these coefficients for the mixture (μ and κ) are taken from Chapman-Enskog theory presented at Reid et al. (1977) with the aid of Wilke approximation and Wassiljewa equation respectively.

Dufour and Soret effects, body force diffusion and self-diffusion are neglected. The only driving force responsible for mass diffusion is the species concentration gradient. Therefore, mass diffusivity is given by the binary diffusion coefficient ($\mathscr{D}_{12}$). This coefficient is calculated using Chapman-Enskog theory presented at Reid et al.(1977) along with Neufeld et al. relation for diffusion collision integral calculations. No pressure dependence is taken into account since for temperature and pressure levels considered pressure does not affect the physical properties (Salemi, 2006).

Heat capacity at constant pressure (c_{p_i}) and sensible enthalpy (h_{sens_i}) for each species are temperature polynomial functions as presented by Zehe et al. (2002), where $i = 1, 2$. Enthalpy is calculated as follows:

$$h_i = \Delta h_{f_i}^{298.15} + \int_{298.15}^{T} c_{p_i} dT, \tag{1}$$

where h_i is the enthalpy of species i, $\Delta h_{f_i}^{298.15}$ is the enthalpy of formation of species i at the reference temperature of $298.15K$ and $\int_{298.15}^{T} c_{p_i} dT$ is the sensible enthalpy of species i, also at the reference temperature of $298.15K$.

So, the enthalpy of the gas can be calculated as presented by Van Wylen et al. (1994) as $h = h_1 Y_1 + h_2 Y_2$, where Y_1 and Y_2 are the mass fractions of the species present in the upper and lower layers respectively.

The Prandtl and Lewis numbers are defined as:

$$Pr = \frac{\mu\, c_p}{\kappa}. \qquad Le = \frac{\kappa}{\rho\, c_p\, \mathscr{D}_{12}}, \tag{2}$$

Prandtl number follows the usual definition, but it is appropriate to make a comment on the Lewis number. This definition is presented by Bejan (1984), Williams (1985), Kuo (1986), Incropera and DeWitt (1998) and Turns (2000). Kuo (1986) mentions that Lewis number can also be defined as the inverse of the equation presented above. Such a definition can be found in the works of White (1974), Kays and Crawford (1983) and Anderson (2000). The definition of this parameter is important as it influences on the governing equations of the problem. Kennedy and Gatski (1994) defined Lewis number as used here but have used the conservation equations taken from Anderson (2000), which the inverse definition. Therefore, some of their results are contradictory as mentioned by Kozusko et al. (1996).

The Chapman-Rubesin parameter comes into play on the development of the similar solution equations presented below. This parameter is defined as:

$$\mathcal{C} = \frac{\rho\, \mu}{\rho_1\, \mu_1}, \tag{3}$$

where $\mathcal{C}$ is nondimensional, ρ is the local density, μ is the local viscosity, ρ_1 is the free stream density of the gas in the upper layer and μ_1 is the free stream viscosity of the gas in the upper layer.

In the present work, only the cases where the velocity ratio is equal to 0.5 are analysed. The velocity and enthalpy ratios, are given by: $\beta_U = U_2/U_1$ and $\beta_h = h_2/h_1$,
where h_1 is the free stream enthalpy of the gas in the upper layer and h_2 is the free stream enthalpy of the gas in the lower layer.

2.2 Similar solution equations

Hydrodinamic stability analysis of the shear layer begins with the calculation of the laminar base flow, as the local normal mode analysis needs the values of the flow variables.

The technique used herein to solve the laminar flow field is the search for a similar solution of the conservation equations through the use of integral coordinate transformations. The transformation used for this task is called Lees-Dorodnitsyn transformation (Anderson, 2000), which is given by:

$$\xi = \int_0^x \rho_1 U_1 \mu_1\, dx, \qquad \eta = \frac{U_1}{\sqrt{2\,\xi}} \int_0^y \rho\, dy, \tag{4}$$

where ξ is the longitudinal direction in the similar space, η is the normal direction in the similar space, x is the longitudinal direction in the physical space, y is the normal direction in the physical space, ρ is the local density, ρ_1 is the free stream density of the gas in the upper layer, U_1 is the free stream velocity of the gas in the upper layer in the x direction and μ_1 is the free stream viscosity of the gas in the upper layer. With the aid of the above equations the physical space $(x, y)$is transformed into a similar space (ξ, η).

Introducing the stream function, ψ, that for a compressible flow is given by:

$$\frac{\partial \psi}{\partial x} = -\rho\, v, \qquad \frac{\partial \psi}{\partial y} = \rho\, u. \tag{5}$$

It is assumed in this development that $\xi = \xi(x)$ only. Lets define three similarity variables given by:

$$\frac{\partial f}{\partial \eta} = \frac{u}{U_1} \equiv f', \qquad g = \frac{h}{h_1}, \qquad s_1 = Y_1. \tag{6}$$

After the previous definitions, the equations to be transformed are presented. These are the conservation equations with the boundary layer assumptions presented by Anderson (2000). They are as follows:

$$\frac{\partial (\rho\, u)}{\partial x} + \frac{\partial (\rho\, v)}{\partial y} = 0, \tag{7}$$

$$\rho\, u \frac{\partial u}{\partial x} + \rho\, v \frac{\partial u}{\partial y} = -\frac{\partial p}{\partial x} + \frac{\partial}{\partial y}\left(\mu \frac{\partial u}{\partial y}\right), \tag{8}$$

$$\frac{\partial p}{\partial y} = 0, \tag{9}$$

$$\rho\, u \frac{\partial h}{\partial x} + \rho\, v \frac{\partial h}{\partial y} = \frac{\partial}{\partial y}\left[\rho\, \mathscr{D}_{12}\left(h_1 \frac{\partial Y_1}{\partial y} + h_2 \frac{\partial Y_2}{\partial y}\right)\right] + \frac{\partial}{\partial y}\left(\kappa \frac{\partial T}{\partial y}\right) + u \frac{\partial p}{\partial x} + \mu \left(\frac{\partial u}{\partial y}\right)^2, \tag{10}$$

$$\rho\, u \frac{\partial Y_1}{\partial x} + \rho\, v \frac{\partial Y_1}{\partial y} = \frac{\partial}{\partial y}\left(\rho\, \mathscr{D}_{12} \frac{\partial Y_1}{\partial y}\right) + \dot{\varpi}, \tag{11}$$

$$p = \rho\, R\, T, \tag{12}$$

where Eq. 7 is the continuity or mass conservation equation, Eq. 8 is the momentum conservation equation in the x direction, Eq. 9 is the momentum conservation equation in the y direction, Eq. 10 is the energy conservation equation, Eq. 11 is the species conservation equation and Eq. 12 is the perfect gas equation of state.

By making the proper substitutions and algebraic manipulations, the following system of ordinary differential equations is obtained:

$$f''' + \frac{f\, f''}{\mathcal{C}} = 0, \qquad g'' + \frac{Pr}{\mathcal{C}}\, f\, g' + \frac{Pr\, U_1^2}{h_1}\,(f'')^2 = 0, \qquad s_1'' + \frac{Le\, Pr}{\mathcal{C}}\, f\, s_1' = 0, \tag{13}$$

These are the similar equations necessary to solve the laminar flow field for the compressible binary plane shear layer problem. The details are explained in the work of Salemi (2006) and the proper boundary conditions are presented below as:

$$\begin{aligned} &f(0) = 0 \qquad f'(+\infty) \to 1 \qquad f'(-\infty) \to \beta_U, \\ &g(+\infty) \to 1 \qquad g(-\infty) \to \beta_h, \qquad\qquad s_1(+\infty) \to 1 \qquad s_1(-\infty) \to 0. \end{aligned} \tag{14}$$

Where the condition $f(0) = 0$ corresponds to $v(0) = 0$ and deservs some additional considerations. The especification of this boundary condition is known as the third bounday condition problem. When a similar solution for the boundary layer problem is sought, the Navier-Stokes equations are transformed into the Blasius equation (Currie, 1974), which is a third order non-linear differential equation. Therefore, from a mathematical point of view, it needs three boundary conditions for its solution.

In the boundary layer problem, the non-slip condition ($u(0) = 0$) and the lack of mass transfer through the wall ($v(0) = 0$) well poses the problem setting two boundary conditions and letting the third to tend to the free stream velocity ($u(\infty) \to U_\infty$). For the shear layer problem, such is not true as there are only two well posed boundary conditions, which are the $u(+\infty) \to U_1$ and $u(-\infty) \to U_2$. So, another condition must be imposed for the problem to be solved. Herein, we assume that $v(0) = 0$, which means that there is no flow through the stream line that leaves the trailing edge of the splitter plate. Different methodologies have been presented in the litterature to address the third boundary condition problem, but this is an open issue. A priory, changing the third boundary condition changes the vertical position of the laminar velocity profiles, but does not change the shape of these profiles or their behavior at $\pm\infty$. Dispite the fact that this is an open question, the approximation $v(0) = 0$ allows a consistent engineering analysis at a low computational cost.

2.3 Linear disturbance equations

The instability present in a shear layer is primarily inviscid (Mack, 1984) and shear stresses have a stabilizing role. Besides that, as pointed out by Ragab and Wu (1989), inviscid stability is an upper limit for the amplification rates of small disturbances, with the viscous ones having lower amplification rates for the same condition. Therefore, linear inviscid stability analysis is performed.

Whenever inviscid stability analyisis is performed, Euler equations are used with the free stream variables nondimensionalized in the same fashion as presented by Planché (1993) using the fast stream on the upper side properties as reference values and the vorticity thickness δ_ω as length scale.

$$\delta_\omega = \frac{\Delta U}{(\partial U/\partial y)_{max}}. \tag{15}$$

where δ_ω is the vorticity thickness.

In order to simplify the notation, on the derivation of the equations used on the linear stability analysis, the symbol * is not carried further to identify a nondimensionalized variable. Therefore, the nondimensionalized Euler equations are:

$$\frac{\partial \rho}{\partial t} + \frac{\partial (\rho\, u)}{\partial x} + \frac{\partial (\rho\, v)}{\partial y} + \frac{\partial (\rho\, w)}{\partial z} = 0, \tag{16}$$

$$\rho \frac{\partial u}{\partial t} + \rho\, u \frac{\partial u}{\partial x} + \rho\, v \frac{\partial u}{\partial y} + \rho\, w \frac{\partial u}{\partial z} = -\frac{1}{\gamma_1\, Ma_1^2} \frac{\partial p}{\partial x}, \tag{17}$$

$$\rho \frac{\partial v}{\partial t} + \rho\, u \frac{\partial v}{\partial x} + \rho\, v \frac{\partial v}{\partial y} + \rho\, w \frac{\partial v}{\partial z} = -\frac{1}{\gamma_1\, Ma_1^2} \frac{\partial p}{\partial y}, \tag{18}$$

$$\rho \frac{\partial w}{\partial t} + \rho\, u \frac{\partial w}{\partial x} + \rho\, v \frac{\partial w}{\partial y} + \rho\, w \frac{\partial w}{\partial z} = -\frac{1}{\gamma_1\, Ma_1^2} \frac{\partial p}{\partial z}, \tag{19}$$

$$\rho \frac{\partial T}{\partial t} + \rho\, u \frac{\partial T}{\partial x} + \rho\, v \frac{\partial T}{\partial y} + \rho\, w \frac{\partial T}{\partial z} = \frac{-p\,(\gamma - 1)}{R} \left(\frac{\partial u}{\partial x} + \frac{\partial v}{\partial y} + \frac{\partial w}{\partial z} \right), \tag{20}$$

$$\rho \frac{\partial Y_1}{\partial t} + \rho\, u \frac{\partial Y_1}{\partial x} + \rho\, v \frac{\partial Y_1}{\partial y} + \rho\, w \frac{\partial Y_1}{\partial z} = 0, \tag{21}$$

$$p = \rho\, R\, T, \tag{22}$$

The mathematical model that describes the evolution of small disturbances within a flow is based on the decomposition of the dependent variables of the flow on a laminar base flow and a small disturbance. Therefore, for the compressible binary shear layer considering local parallel flow, no laminar flow velocity components in the y and z directions and uniform pressure field, we have:

$$u(x,y,z,t) = \bar{u}(y) + u'(x,y,z,t), \quad v(x,y,z,t) = v'(x,y,z,t), \quad w(x,y,z,t) = w'(x,y,z,t), \tag{23}$$

$$\rho(x,y,z,t) = \bar{\rho}(y) + \rho'(x,y,z,t), \quad T(x,y,z,t) = \overline{T}(y) + T'(x,y,z,t), \tag{24}$$

$$p(x,y,z,t) = 1 + p'(x,y,z,t), \qquad Y_1(x,y,z,t) = \overline{Y_1}(y) + Y_1{}'(x,y,z,t). \tag{25}$$

Now it is possible to propose a normal mode form of solution for the small disturbances, represented by:

$$u', v', w', \rho', T', p', Y_1{}'(x,y,z,t) \;= \Re \left\{ \left(\hat{u}, \hat{v}, \hat{w}, \hat{\rho}, \widehat{T}, \hat{p}, \widehat{Y_1} \right)(y) \exp\left[\, i\,(\,\alpha x + \beta z - \omega t\,)\,\right] \right\}, \tag{26}$$

where the variables identified with a hat $\hat{}$ are the eigenfunctions of the dependent variables of the flow, α is real and the wave number in the x direction, β is real and the wave number in the z direction and ω is complex and the angular frequency of the disturbance.

By making the appropriate substitutions, manipulating and linearizing the resulting equations, the following stability equations are obtained:

$$\hat{\rho}\, i\,(\alpha\bar{u} - \omega) + \hat{v}\, \frac{d\bar{\rho}}{dy} + \bar{\rho} \left[i\,(\alpha\hat{u} + \beta\hat{w}) + \frac{d\hat{v}}{dy} \right] = 0, \qquad \bar{\rho} \left[i\,(\alpha\bar{u} - \omega)\,\hat{u} + \hat{v}\, \frac{d\bar{u}}{dy} \right] = -\frac{i\alpha\hat{p}}{\gamma_1\, Ma_1^2}, \tag{27}$$

$$\bar{\rho}\, i\,(\alpha\bar{u} - \omega)\,\hat{v} = -\frac{1}{\gamma_1\, Ma_1^2}\, \frac{d\hat{p}}{dy}, \qquad \bar{\rho}\, i\,(\alpha\bar{u} - \omega)\,\hat{w} = -\frac{i\beta\hat{p}}{\gamma_1\, Ma_1^2}, \tag{28}$$

$$\bar{\rho}\left[i\left(\alpha\bar{u}-\omega\right)\widehat{T}+\hat{v}\,\frac{d\overline{T}}{dy}\right]=-\frac{(\gamma-1)}{R}\left[i\left(\alpha\hat{u}+\beta\hat{w}\right)+\frac{d\hat{v}}{dy}\right], \tag{29}$$

$$\bar{\rho}\left[i\left(\alpha\bar{u}-\omega\right)\widehat{Y}_1+\hat{v}\,\frac{d\overline{Y}_1}{dy}\right]=0\,,\qquad \hat{p}=\bar{\rho}\,R\,\widehat{T}+\hat{\rho}\,R\,\overline{T}\,. \tag{30}$$

With the aid of the transformation introduced by Gropengiesser (1970) given by the χ function, the stability equations can be condensed into only one ordinary differential equation:

$$\chi=\frac{i\alpha\hat{p}}{\gamma_1\,Ma_1^2\,\hat{v}},\qquad \frac{d\chi}{dy}=\frac{\alpha^2\left(\bar{u}-\omega/\alpha\right)}{R\overline{T}}-\chi\left[\frac{\chi G+(d\bar{u}/dy)}{(\bar{u}-\omega/\alpha)}\right], \tag{31}$$

with the following boundary condition:

$$\chi\left(y\to\pm\infty\right)=\mp\frac{\alpha\left(\bar{u}-\omega/\alpha\right)}{\sqrt{G\,R\overline{\overline{T}}}}\,,\qquad G=\frac{\alpha^2+\beta^2}{\bar{\rho}\,\alpha^2}-Ma_1^2\,\frac{\gamma_1}{\gamma}\,\frac{\left(\alpha\bar{u}-\omega\right)^2}{\alpha^2}\,. \tag{32}$$

3. RESULTS

For the hydrodynamic stability study of the compressible shear layer, it is mandatory that the system of coupled similarity differential equations be solved to generate the laminar base flow properties profiles. This task is perfomed by a software programmed in FORTRAN language by the authors and called `Coupled1.f`. The base flow profiles are then supplied to another software, also programmed in FORTRAN language by the authors and called `Stability3A.f`, which performs the inviscid temporal linear stability analysis. These codes are well explained in the work of Salemi (2006), along with the numerical methods employed and calculation tolerances used.

3.1 Codes verification

In order to verify the calculations performed by the codes `Coupled1.f` and `Stability3A.f` the following analysis were performed:

1. `Coupled1.f`: Validation of the similar solution through a comparison of the calculated longitudinal base flow velocity profile, u, for the incompressible case with the analytical error function profile presented by Lardjane et al. (2004) and also a comparison of the similar functions f, f' e f'' calculated for higher convective Mach numbers, with the data presented by Kennedy and Gatski (1994);

2. `Stability3A.f`: Validation of the temporal stability calculation of the temporal amplification rates with the ones obtained by Michalke (1964), Sandham (1990) and Shin (1991);

Lardjane et al. (2004) presented an analytical expression for the longitudinal velocity for a monospecies isothermal incompressible shear layer, which is a limit case of our analysis. This relation is given by:

$$u=\frac{\Delta U}{2}\,\mathrm{erf}\left(\sqrt{\pi}\,\frac{y}{\delta_\omega}\right). \tag{33}$$

where erf is the error function and ΔU is the velocity difference. This relationship was used for a N_2 - N_2 shear layer at $1\,atm$ and $T_1=T_2=300\,K$. Velocity data for each layer are $U_1=30\,m/s$, $U_2=10\,m/s$ with $M_C=0.028$.

It can be seen that the numerical results of `Coupled1.f` for the incompressible case match the analytical expression presented by Lardjane et al. (2004).

For higher convective Mach numbers, the calculated data for the similar functions f, f' and f'' are compared with those presented by Kennedy and Gatski (1994) for a H_2 - N_2 shear layer at $49000\,Pa$ and temperatures $T_1=215\,K$ and $T_2=334\,K$. The convective Mach numbers analysed were 0.20, 0.70 and 1.20.

By analysing Figs. 6 through 8 it is possible to notice that the agreement with Kennedy and Gatski (1994) data is quite good, considering the fact that their data had to be digitized for this comparison to be made. It is also necessary to mention that Kennedy and Gatski (1994) did not use the third condition as $v(0)=0$. So, the position in η of the velocity similarity functions profile had to be corrected on the presentation of the data. It is noticeable that f presents almost the same results, f' presents a small difference in the lower layer and f'' maxima are somewhat different. These differences can be associated with the fact that Kennedy and Gatski (1994) used in their formulation $\mathcal{C}$, Pr and Le variable through the layer, whereas in the present work these parameters are constant and equal to 1.

Michalke (1964) performed temporal stability calculations for a analytical velocity profile given by $U(y)=0.5\,[\,1+\tanh(y)\,]$. Sandham (1990) used these data in his verification and so did Shin and Ferziger (1991). Therefore, calculations using this velocity profile were performed to verify the method used by `Stability3A.f`. The results are presented below in Fig. 9 and show very good agreement with the data provided by Michalke (1964), Sandham (1990) and Shin and Ferziger (1991).

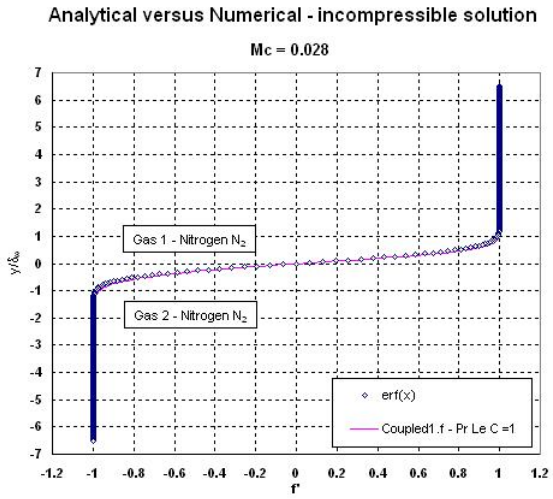

Figure 5. N_2 - N_2 incompressible shear layer: Analytical versus numerical solution

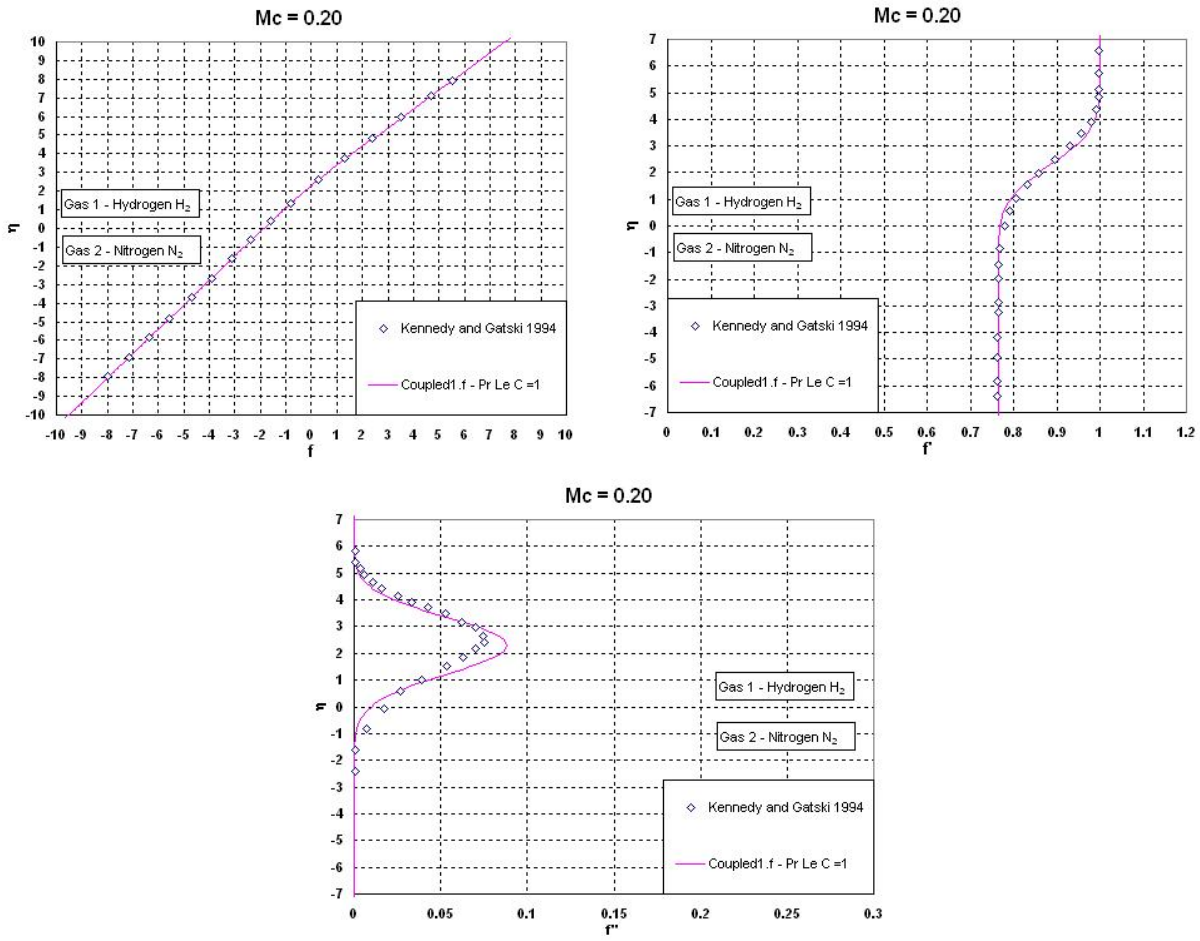

Figure 6. Similarity functions for H_2 - N_2 shear layer and $M_C = 0.20$

3.2 Parametrical study of $\mathcal{C}$, Pr and Le variations

This part of the work was performed making two parameters equal to 1 and letting the other one to vary within a given range. Such analysis allowed to investigate the influence of the variations of $\mathcal{C}$, Pr and Le on the laminar base flow properties profiles and also on the temporal stability amplification rates of small disturbances on a compressible binary shear layer. For a O_2 - H_2 shear layer at $300K$, $1\,atm$, $U_1 = 1846\,m/s$, $U_2 = 200\,m/s$ and $M_C = 1.00$ laminar base flow properties profiles were calculated and plotted. In the work of Salemi (2006), a parametric study was performed in

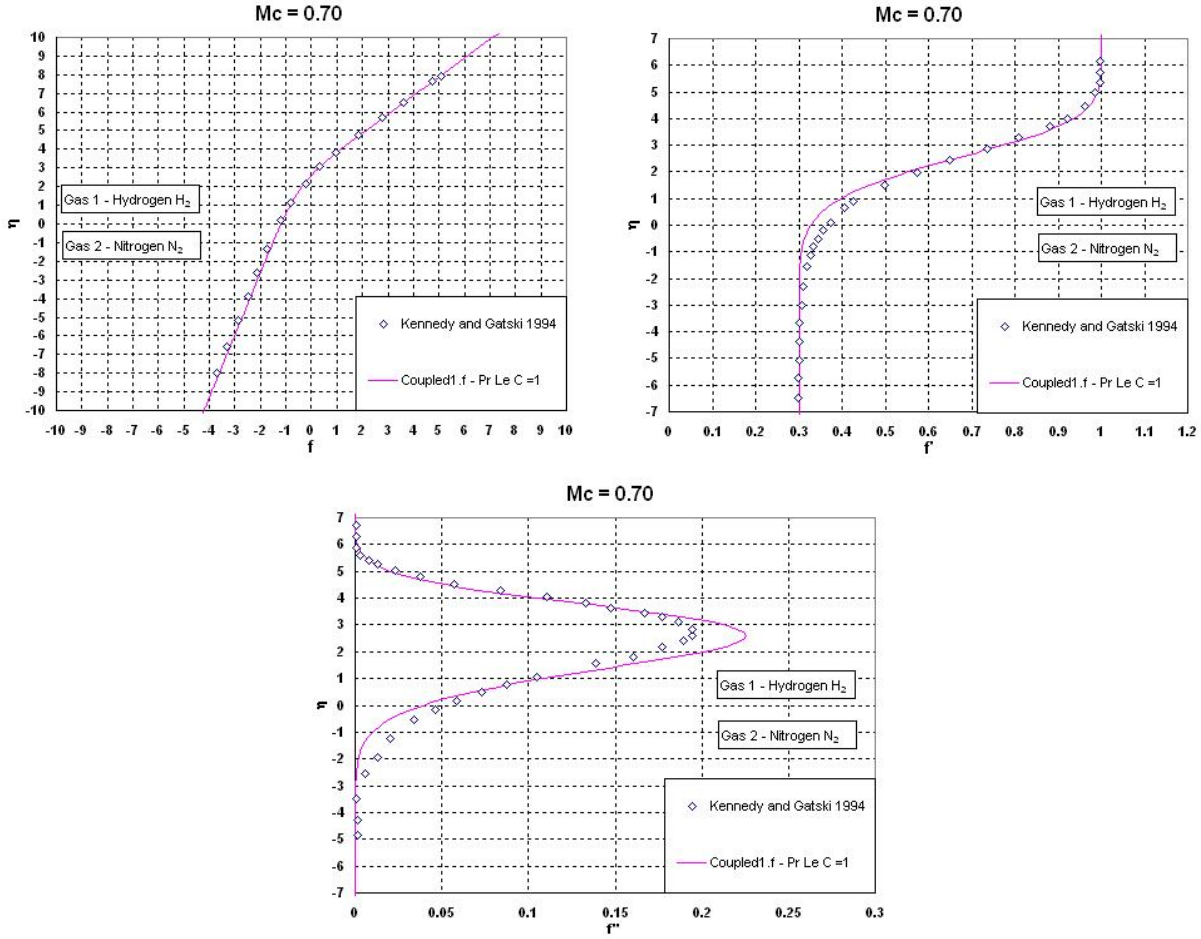

Figure 7. Similarity functions for H_2 - N_2 shear layer and $M_C = 0.70$

order to guide the chosen ranges of $\mathcal{C}$, Pr and Le.

Figure 10 shows that the Prandtl number does not affect the bounds of the velocity profile. Such behavior is explained if the equation for the similarity function f is examined. There is no Pr dependence on this equation. But temperature and mass fraction profiles are both affected by Pr variations. A increase in Pr reduces the thermal boundary layer, which means that heat is being less diffused than momentum. As a consequence the temperature rises inside the layer. The case where $Pr = 1.3$ presents a temperature peak almost $2\,\%$ higher than for the case where $Pr = 1.0$. If $Pr = 0.4$ the temperature peak is almost $5\,\%$ lower than for the case where $Pr = 1.0$. It is also noticed that increasing Pr decreases the bounds of the mass fraction profiles.

The effect of Lewis number is presented on Fig. 11. It is shown that the bounds of the velocity profile are also not affected. Again, temperature and mass fraction profiles are both affected by Le variations. It is noticed that an increasing Lewis number decreases the bounds of thermal boundary layer and an additional effect of maxima displacement towards the fast O_2 stream. Concentration boundary layer also decreases its thickness with a increase in Le. For the cases presented herein, the mass fraction profile tail is longer on the slower H_2 stream. Compared to $Le = 1.0$ case, temperature peaks are almost $11\,\%$ higher for the case where $Le = 2.3$ and almost $1.5\,\%$ lower when $Le = 0.3$.

On Fig. 12 are presented the results for the effect of the Chapman-Rubesin parameter. Differently from the Lewis and Prandtl number, variations on the Chapman-Rubesin parameter , $\mathcal{C}$, affect the velocity profiles. It can be seen that increasing this parameter results in an increase of the bounds of the velocity profiles towards the fast and slow sides, but with a pronounced effect on the slow side. It is interesting to observe that when $\mathcal{C} = 0.01$, the profiles turn to be very slender. Other peculiar aspect, is the spreading of the thermal layer towards both layers and a displacement of its maxima to the fast O_2 layer. Although, the temperature peak remains unchanged. Mass fraction profiles follow the same tendency as velocity ones.

In order to evaluate the influence of the variations of $\mathcal{C}$, Pr and Le on the temporal stability amplification rates of small disturbances a N_2 - O_2 shear layer at $300K$, $1\,atm$, $U_1 = 1370\,m/s$, $U_2 = 685\,m/s$ and $M_C = 1.00$ was analysed. Although not presented, the effect of such parameters for $M_C = 0.01$ was calculated and considered negligible. Therefore, it can be stated that increasing compressibility implies in greater influence of the variations of $\mathcal{C}$, Pr and Le in

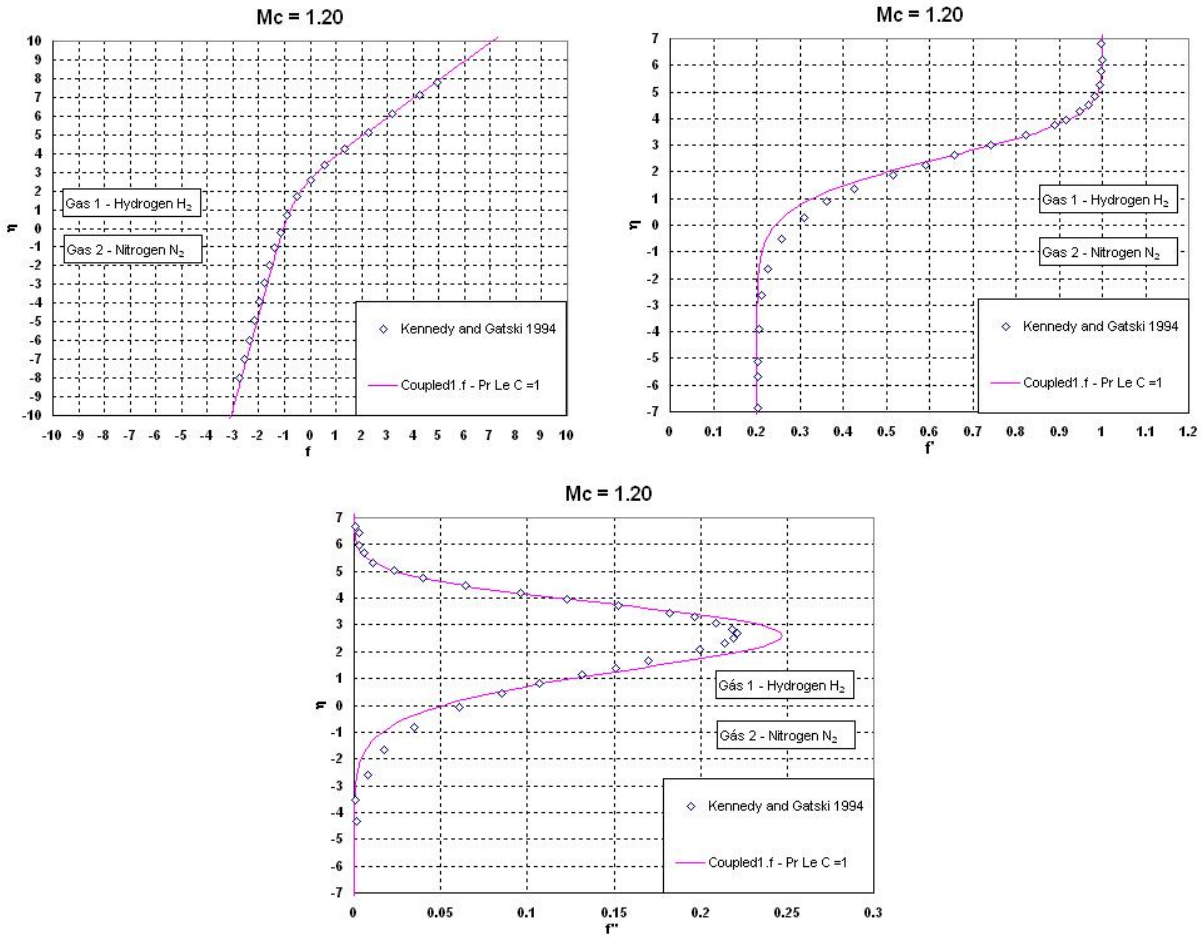

Figure 8. Similarity functions for H_2 - N_2 shear layer and $M_C = 1.20$

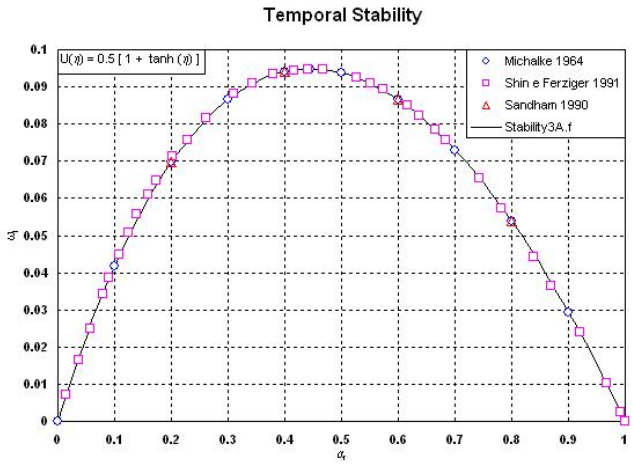

Figure 9. Temporal stability analysis with analytical velocity profile $U(y) = 0.5\,[1 + \tanh(y)\,]$ - Comparison with data provided by Michalke (1964), Sandham (1990) and Shin and Ferziger (1991)

the amplification rates.

It can be seen on Fig. 13 that incresing Prandtl number, the maximum temporal amplification rate ($\omega_i^{\max}$) decreases along with amplification rates for other wave numbers (α_r). Although the neutral wave number (α_r^0) was not calculated, by observing Fig.13 it can be inferred that increasing Pr decreases α_r^0. But for $Pr > 1$, α_r^0 seems to increase, expanding the range of unstable wave numbers. Figure 13 also shows that for wave numbers higher than the wave number with maximum amplification rate($\alpha_r^{\max}$), increasing Lewis number makes the amplifications rates to decrease. For the values of Le analysed, when $Le > 1$ the amplification rates start to grow again.

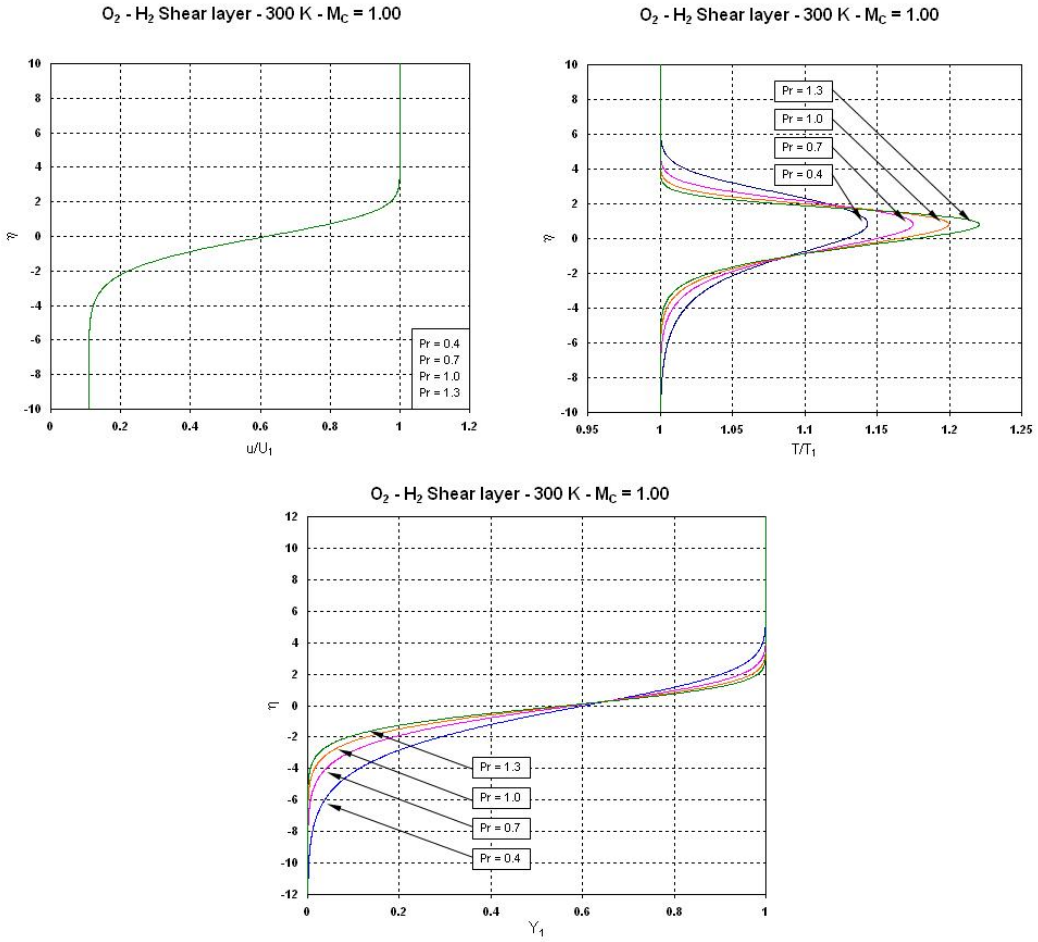

Figure 10. Effect of the Prandtl number, Pr, for a O_2 - H_2 shear layer

In the case of Chapman-Rubesin parameter, it is shown on Fig.13 that except for $\mathcal{C} = 0.01$, the amplification rates increase for all wave numbers, but the ranges of unstable wave numbers are almost unchanged. It is noticeable that from $\mathcal{C} > 5.0$ to $\mathcal{C} < 30.0$, amplification rates increase in a lesser rate than from $\mathcal{C} > 1$ para $\mathcal{C} < 5$.

3.3 Results for different convective Mach numbers

Temporal stability analysis were performed for various convective Mach numbers and non-oblique waves. The results are presented in Fig. 14. It is noticed that the temporal amplification rates of non-oblique waves decrease when convective Mach number increases. This is one of the negative effects of the compressibility as results in a later transition to turbulent flow, which is not interesting for a SCRAMJET. Interesting is the fact that, for the convective Mach numbers analysed from $M_C = 0.9$ to $M_C = 1.1$ the curves start to present two peaks. This phenomena is somewhat curious. It suggests some change in the flow pattern and permits an analogy to aerodynamics to coin the term transonic convective Mach number. Although, no additional instability modes as the ones found by Mack (1984) and others were found. For this range of convective Mach numbers the bandeidth of unstable wave numbers stop to become narrower as the temporal amplification rates decreases. After $M_C = 1.4$ it was noticed that, although the maximum amplification rate decreases, the range of unstable wave numbers increase.

4. CONCLUSIONS

Linear stability analysis is a technique which has proven its applicability to many problems in fluid mechanics. Herein, it was applied to the compressible binary shear layer where it was possible to identify some tendencies and characteristics of the physics of the problem. This study is applicable to the research of basic supersonic combustion and represents the beginning of more sophisticated studies such as the control of supersonic reactive flows.

Influence of the variations of $\mathcal{C}$, Pr and Le on the laminar base flow properties profiles and also on the temporal stability amplification rates of small disturbances were investigated. These evaluations shown that using these parameters as constants and equal to 1, which is the most common assumption, can result in noticeable differences on the physical

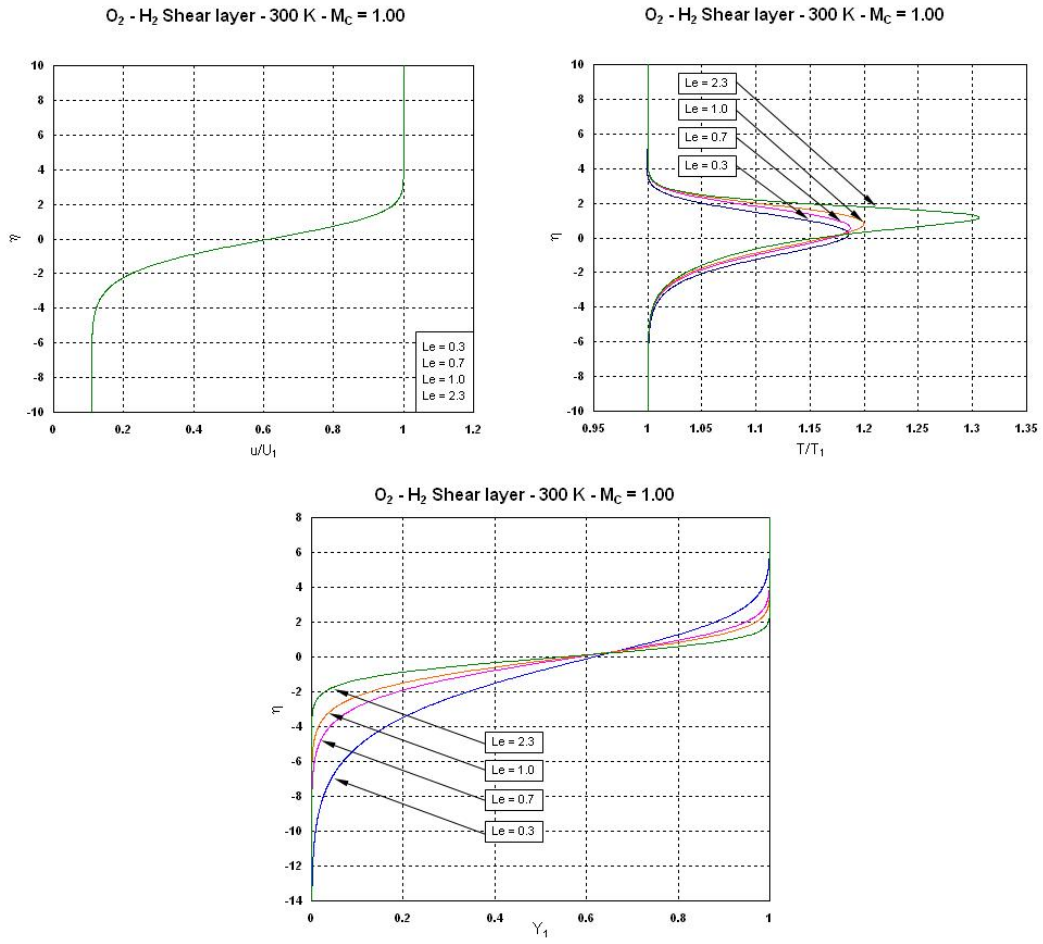

Figure 11. Effect of the Lewis number, Le, for a O_2 - H_2 shear layer

aspects of the shear layer and also on different stability properties.

Data for convective Mach numbers from 0.01 to 1.6 were generated and confirmed the tendency presented in the literature that the temporal amplification rates of non-oblique waves decrease when convective Mach number increases.

Based on what was presented, it is possible to comment some points. Up to now, the shear layer problem still poses some challenges like the third boundary condition problem. Due to the quantity of variables present on the problem, the present work must be extended. So, other relevant aspects such as different velocity and temperature ratios can be better evaluated. It is also the first step to develop a code capable of performing reactive shear layer analysis, which is an essential asset when designing a supersonic combustion ramjet engine and flow control strategies.

5. REFERENCES

Anderson, J.D., 2000, "Hypersonic and high temperature gas dynamics", AIAA, U.S.A.

Bejan, A., 1984, "Convection heat transfer", John Wiley & Sons, Inc., U.S.A.

Brown, G.L. and Roshko, A., 1974, "On density effects and large structure in turbulent mixing layers", Journal of Fluid Mechanics, Vol. 64, pp. 775-781.

Currie, I.G., 1974, "Fundamental mechanics of fluids", Mcgraw Hill, Inc, U.S.A.

Fedioun, I. and Lardjane, N., 2005, "Temporal linear stability analysis of three-dimensional compressible binary shear layers", AIAA Journal, Vol. 43, No. 1, pp. 111-123.

Gropengiesser, H., 1970, "Study on the stability of boundary layers in compressible fluids", NASA Technical Translation, No. F-12, National Aeronautics and Space Administration, U.S.A.

Incropera, F.P. and DeWitt, D.P., 1998, "Fundamentos de transferência de calor e de massa", Livros Técnicos e Científicos Editora S.A., Brazil.

Kays, W.M. and Crawford, M.E., 1983, "Convective heat and mass transfer", Mcgraw Hill, Inc, U.S.A.

Kennedy, C.A. and Gatski, T.B., 1994, "Self-similar supersonic variable-density shear layers in binary systems", Physics of Fluids, Vol. 6, No. 2, pp. 662-673.

Kozusko, F., Grosch, C.E., Jackson, T.L., Kennedy, C.A. and Gatski, T.B., 1996, "The structure of a variable property,

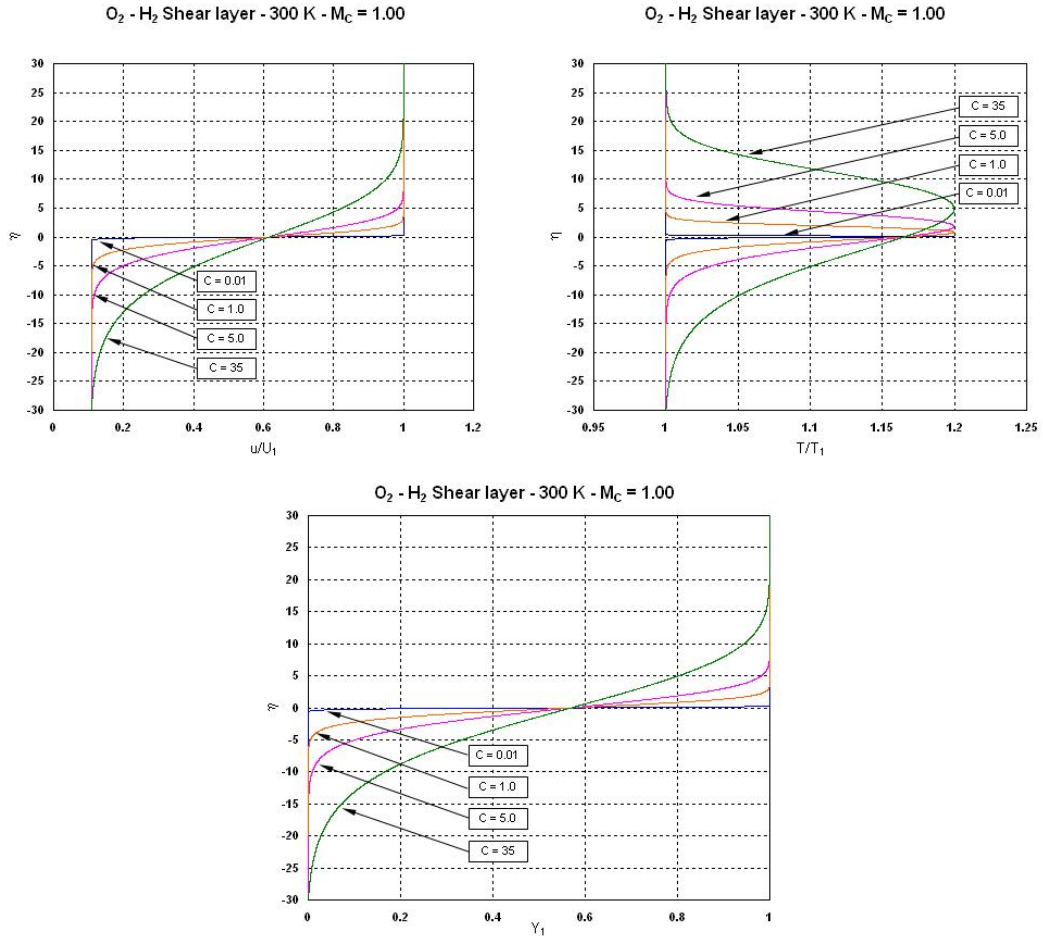

Figure 12. Effect of the Chapman-Rubesin parameter, $\mathcal{C}$, for a O_2 - H_2 shear layer

compressible mixing layers in binary gas mixtures", Physics of Fluids, Vol. 8, No. 7, pp. 1945-1953.

Kuo, K.K., 1986, "Principles of combustion", Wiley-Interscience, John Wiley & Sons, Inc., U.S.A.

Lardjane, N., Fedioun, F. and Gökalp, I., 2004, "Accurate initial conditions for the direct numerical simulation of temporal compressible binary shear layers with high density ratio", Computers & Fluids, Vol. 33, pp. 549-576.

Mack, L.M., 1984, "Boundary layer linear stability theory", AGARD Special Course, Pasadena, California: Jet Propulsion Laboratory. California Institute of Technology, U.S.A.

Michalke, A., 1964, " On the inviscid instability of the hyperbolic-tangent velocity profile", Journal of Fluid Mechanics, Vol. 19, pp. 543-556.

Merry, J., 2006, "The Aviation History Online Museum", http://www.aviation-history.com/engines/ramjet.htm.

Planché, O.H.R., 1993, "A numerical investigation of the compressible reacting mixing layer", Ph.D. Thesis, Department of Mechanical Engineering, Stanford University, Stanford, California, U.S.A.

Ragab, S.A. and Wu, J.L., 1989, "Linear instabilities in two-dimensional compressible mixing layers", Physics of Fluids, Vol. A1, No. 6, pp. 957-966.

Reid, R.C., Prausnitz, J.H. and Sherwood, T.K., 1977, "The properties of gases and liquids", Mcgraw Hill, Inc, U.S.A.

Salemi, L.C., 2006, "Análise de Estabilidade Linear de Camada de Mistura Compressível Binária", Master Thesis, INPE, S.J.Campos, Brazil, 216 p.

Sandham, N.D., 1990, "A numerical investigation of the compressible mixing layer", Ph.D. Thesis, Department of Mechanical Engineering, Stanford University, Stanford, California, U.S.A.

Shin, D.S. and Ferziger, J.H., 1991, "Linear stability of the reacting mixing layer", AIAA Journal, Vol. 29, No. 10, pp. 1634-1642.

Svehla, R.A., 1995, "Transport coefficients for the NASA Lewis chemical equilibrium program", NASA Technical Memorandum, No. 4647, Cleveland, Ohio: National Aeronautics and Space Administration. Lewis Research Center, U.S.A.

Turns, S.R., 2000, "An Introduction to combustion: concepts and applications", McGraw Hill Higher Education, U.S.A.

Van Wylen, G., Sonntag, R. and Borgnakke, C., 1994, "Fundamentos da termodinâmica clássica", Editora Edgar Blücher LTDA., Brazil.

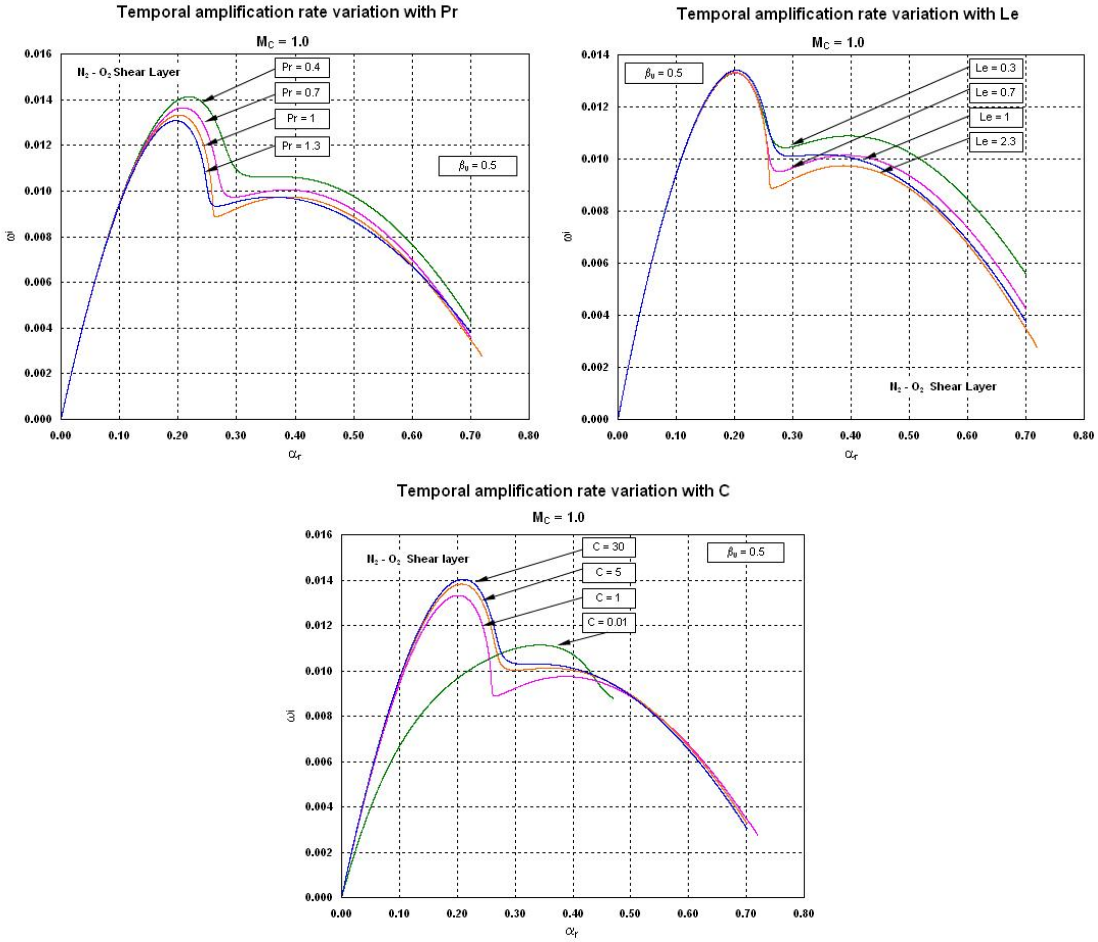

Figure 13. Influence of the variations of $\mathcal{C}$, Pr and Le on the temporal stability amplification rates of N_2 - O_2 shear layer

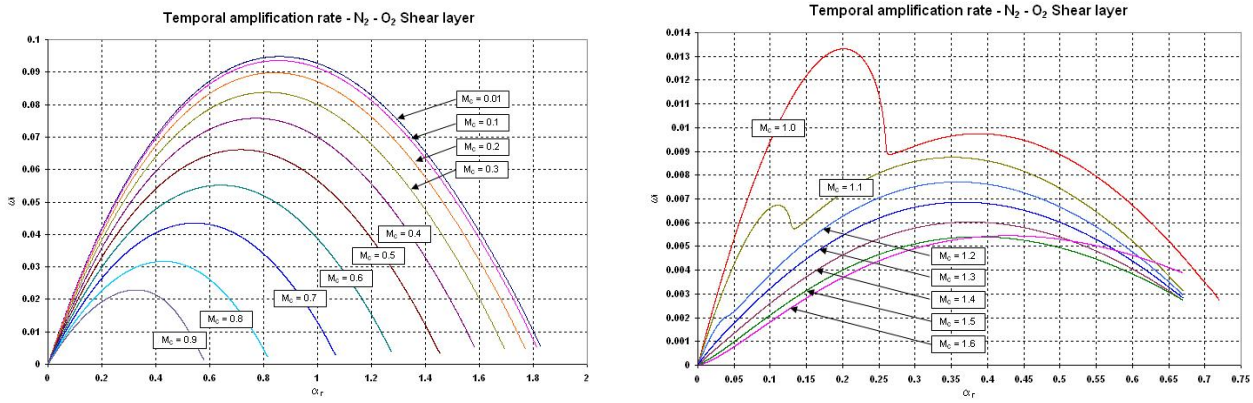

Figure 14. Influence of the variation of M_C on the temporal stability amplification rates of a N_2 - O_2 shear layer

Williams, F.A., 1985, "Combustion theory: the fundamental theory of chemically reacting flow systems", Addison-Wesley Publishing Company, U.S.A.

Winant, C.D. and Browand, F.K., 1974, " Vortex pairing: the mechanism of turbulent mixing layer growth", Journal of Fluid Mechanics, Vol. 63, pp. 237-255.

White, F.M., 1974, "Viscous fluid flow", Mcgraw Hill, U.S.A.

Zehe, M.J., Gordon, S. and McBride, B.J., 2002, "CAP: A computer code for generating tabular thermodynamic functions from NASA Lewis coefficients", NASA TTechnical Publication, No. TP-2001-210959/REV1, Cleveland, Ohio: National Aeronautics and Space Administration. Glenn Research Center, U.S.A.